Nanoscale

Accepted Manuscript

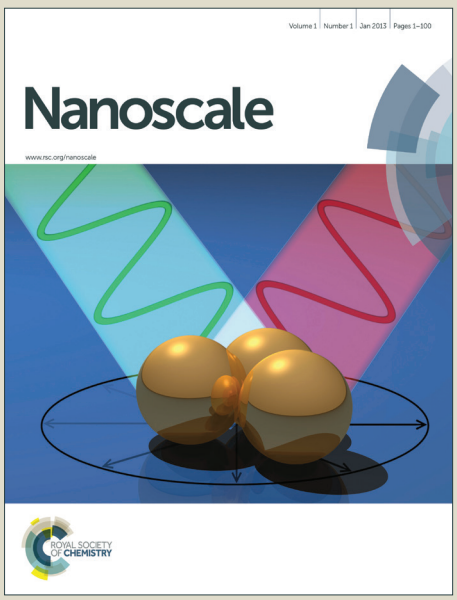

ROYAL SOCIETY OF CHEMISTRY

www.rsc.org/nanoscale

Journal Name

RSCPublishing

COMMUNICATION

Efficient Visible Light-Driven H_2 Production in Water by CdS/CdSe Core/Shell Nanocrystals and Ordinary Nickel-Sulfur Complex

Cite this: DOI: 10.1039/x0xx00000x

Received 00th January 2012,
Accepted 00th January 2012

DOI: 10.1039/x0xx00000x

www.rsc.org/

Ping Wang,[a] Jie Zhang,[a] Haili He,[a,b] Xiaolong Xu[a] and Yongdong Jin[a]*

Solar energy conversion to hydrogen has gained tremendous interests due to its great potential in solving the problem of energy crisis. Among different ways to achieve the goals of H_2 photogeneration, the quantum dots (QDs)-based multicomponent system has been proven to be one of the most prominent methods. Although significant advances have been made recently, the developing of a practical visible light-driven hydrogen generation system with high efficiency and low-cost is still challenging. In this work, we report that a highly active catalyst could be simply obtained through the complexing of nickel ions with S^{2-} or 3-mercaptopropionic acid, and after further combination it with the carefully designed CdS/CdSe core/shell nanocrystals, the aqueous system exhibits a good stability and high efficiency for the H_2 photogeneration. It is expected that our findings would provide new insights for the facile construction of highly efficient and cost-effective solar H_2 generation system for practical applications.

Hydrogen (H_2) as a clean and highly efficient fuel, its production by solar energy has been one of the most active research areas for decades.[1, 2] Considered as an effective route, the semiconductor quantum dots (QDs)-based multicomponent H_2-producing artificial (HPA) system is of great interests for the efficient light-driven reduction of **proton** to H_2 very recently.[3-16] Semiconductor QDs due to its good photostability, consecutive tunable optical properties and large cross-sections across the whole visible region have been elected as the light absorber in these systems.[3, 7] As a QDs-type light absorber, the core/shell QDs is superior to the single component QDs, since the charge recombination and trapping, considered as the processes that will decrease catalytic activity, can be effectively inhibited through the proper shell coating. For instance, Larsen et al. reported that the hydrogen generation activity of the CdSe/CdS core/shell QDs is 10-fold higher than the CdSe QDs, and they attributed this to the passivation of surface-deep trap states of CdSe core by the CdS shell coating.[17] Besides, the CdSe/CdS dot-in-rod nanorods also exhibit the higher photocatalytic activity compared with that of single component CdS nanorods, which is considered to be due to the **increase** of the charge separation through the formation of herterostructures.[3, 13, 18] Therefore, it is expected that the employing of proper core/shell QDs as the light absorber would significantly enhance the activity of **the** HPA system.

In addition to the light absorber, the catalyst is another key factor that would influence the overall efficiency of the HPA system, and various catalysts have been developed for the purpose of increasing the efficiency of **the** HPA system.[19-21] Among of them, the hydrogenases[4, 5] and its mimics,[11, 12] and artificial molecules such as cobaloximes[8, 14] and nickel thiolates[6, 7, 22] have gained great interests due to their relatively high efficiency for H_2 evolution and low cost. Despite of significant advances for the solar energy conversion to H_2 in these works, some obstacles still exist toward the practical applications of the QDs-based HPA systems, such as the instability upon the light irradiation,[4, 5, 11, 12] the moderate conversion efficiency,[4, 11, 12, 14] and the complexity in both catalyst synthesis and further modification onto the surface of QDs.[6-8, 11, 12, 14, 22] Thus, the development of a facile method to construct QDs-based HPA system with high efficiency and good stability is highly desirable.

Herein, we construct a new aqueous H_2 production system that uses CdS/CdSe core/shell QDs as the light absorber, an ordinary nickel-sulfur complex simply obtained by the complexing of Ni^{2+} with S^{2-} (or 3-mercaptopropionic acid, 3-MPA) as the catalyst, and ascorbic acid (AA) as the electron donor. Under optimal conditions, the system exhibits a good stability and achieves the quantum yield of ~ 20.6% under illumination at 520 nm. Detailed studies identify that both nickel and sulfur are indispensable elements for the high activity of the catalyst and the ratio of them has been demonstrated

to significantly influence the H_2 production activity of the HPA system.

As mentioned above, the activity of CdSe/CdS core/shell QDs will be greatly enhanced compared with that of CdSe QDs. However, it should be noted here that the CdSe/CdS core/shell QDs is a typical type-I QDs, where the energy of the conduction band (CB) and valence band (VB) of CdS shell is higher and lower than that of CdSe core, respectively. Hence, the electrons and holes generated in both CdSe and CdS will be removed away from the surface and confined in the core, and thus the activity will be apparently reduced though the charge carriers **that** could tunneling to the surface of QDs to contribute to the proton reduction.[8, 17] On the contrary, CdS/CdSe core/shell QDs, known as **the** reverse type-I QDs, which is with the reverse band alignment compared with that of CdSe/CdS core/shell QDs, is considered could well solve this problem. To test our hypothesis, we synthesized CdSe/CdS and CdS/CdSe core/shell QDs with nearly the same core and overall sizes [23, 24] (see details in ESI and Fig. S1†), and then investigated their activity under the same conditions. For convenience, the CdSe/CdS and CdS/CdSe core/shell QDs are denoted as the **1**-QDs and **2**-QDs in our work, respectively.

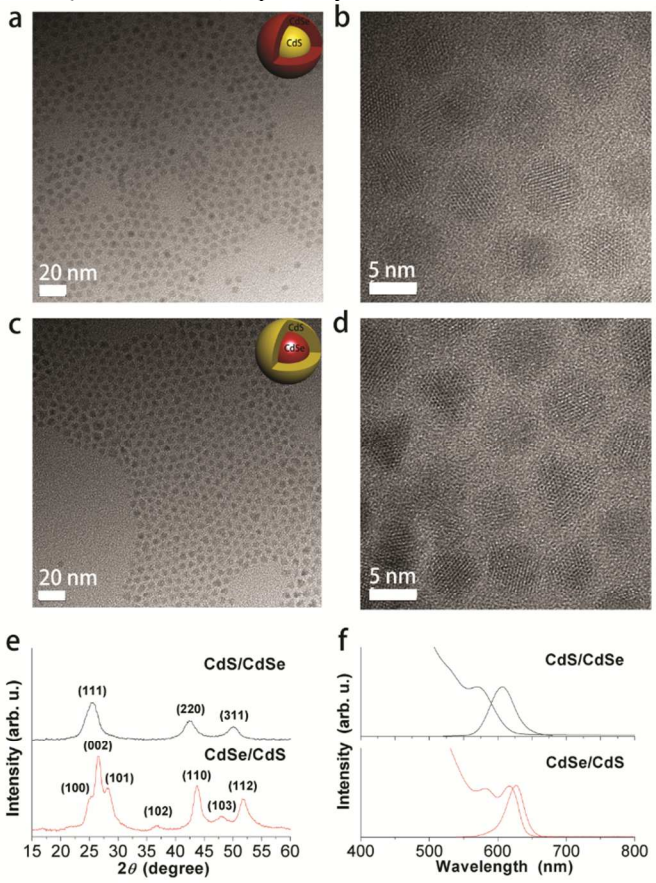

Fig. 1 a, TEM and **b**, HRTEM images of **2**-QDs, respectively. The inset of **a** is the scheme illustration of **2**-QDs. **c**, TEM and **d**, HRTEM images of **1**-QDs, respectively. The inset of **c** is the scheme illustration of **1**-QDs. The scale bars of TEM and HRTRM image are 20 and 5 nm, respectively. The mean sizes of **2**- and **1**-QDs, calculated from the average size of more than 100 single particle in the TEM (**a** and **b**) images, are 5.5 and 5.8 nm, respectively. **e**, XRD patterns of the as-prepared **2**- and **1**-QDs, respectively. **f**, UV-Vis and PL spectra of the as-prepared **2**- and **1**-QDs, respectively.

Fig. 1a-d represent **the** typical transmission electron microscopy (TEM) and corresponding high-resolution TEM (HRTEM) images of the organic ligands capped **2**- and **1**-QDs, with a good crystallinity and the mean size of ~ 5.5 and 5.8 nm, respectively. X-ray diffraction spectra (Fig. 1e) reveal that the prepared **2**- and **1**-QDs are in zinc-blend and wurtzite structure, respectively. The UV-Vis and PL spectra (Fig. 1f) indicates that the first exciton absorption peak and emission peak of **2**-QDs are 571 and 607 nm, respectively; while for that of **1**-QDs are 617 and 627 nm, respectively. For the aqueous-based H_2 generation, two essential points are required for QDs: one is that the QDs should be water-dispersible; while the other is that the ligands on QDs cannot block charge transfer out of them. The recently reported method that using metal-free inorganic ligands to replace original organic ligands on QDs well revolved the above mentioned problems.[25, 26] In our work, two types of QDs capped with different inorganic ligands were synthesized according to that method, and for convenience, **2**-QDs capped with S^{2-} and OH^- is denoted as **2**(S^{2-})- and **2**(OH^-)-QDs, respectively; **1**-QDs capped with S^{2-} is denoted as **1**(S^{2-})-QDs. (see details in the ESI and Fig. S2†).

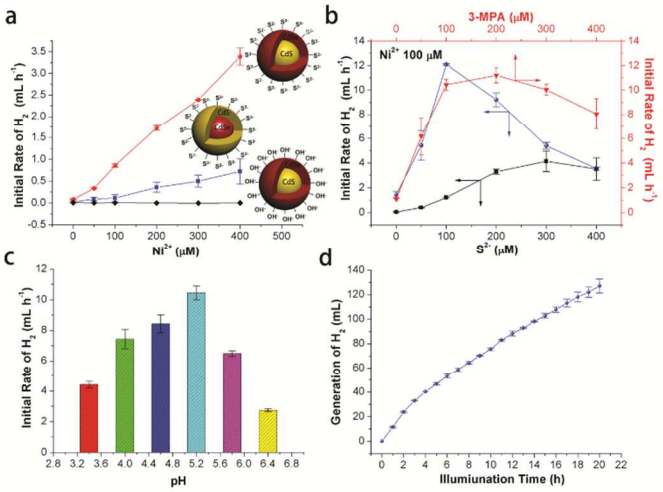

Fig. 2 a, the dependence of $r_{init.}$ of the system containing the same concentration (0.075 μM) of QDs [**2**(S^{2-})-, **1**(S^{2-})- and **2**(OH^-)-QDs] with the conditions of 0.8 M ascorbic acid (AA) at pH 5.2, on the concentration of Ni^{2+}. **b**, $r_{init.}$ of the system with 0.075 μM **2**(OH^-)-QDs (black square) and 0.075 μM **2**(S^{2-})-QDs (blue ball) under conditions of 0.8 M AA, 100 μM Ni^{2+} at pH 5.2 versus the concentration of S^{2-}, respectively; $r_{init.}$ of the system with 0.075 μM **2**(S^{2-})-QDs (red triangle) under conditions of 0.8 M AA, 100 μM Ni^{2+} at pH 5.2 versus the concentration of 3-MPA. **c**, **the** dependence of the initial rate of H_2 generation of the system on pH value with the conditions of 0.075 μM **2**(S^{2-})-QDs, 100 μM Ni^{2+}, 100 μM 3-MPA, 0.8 M AA, pH 5.2 and λ > 420 nm. **d**, the generation of H_2 of the **system** with conditions of 0.075 μM **2**(S^{2-})-QDs, 100 μM Ni^{2+}, 100 μM 3-MPA and 0.8 M AA at pH 5.2 versus illumination time.

H_2 evolution experiments were performed on an airtight inner gas circulation system connected with a gas chromatography that could realize the online quantitative detection of H_2. After degassing process, the colloidal solution was illuminated by a Xenon lamp equipped with the filter of λ > 420 nm or λ = 520 nm. The total volume of the reaction solution in our system is 50 mL. The conditions employed in our H_2 evolution experiments are 0.075 μM QDs, 0.8 M AA, pH 5.2 unless specified. During the choice of catalyst, as the nickel thiolates have been demonstrate to be an effective catalyst for the QDs-based HPA system,[6, 7, 22] we questioned ourselves that whether the composite only with nickel and sulfur element could also possess the similar activity as that of

nickel thiolates. Therefore, we simply introducing Ni^{2+} ions ($Ni(NO_3)_2$) into the system containing different types of QDs (**2**(S^{2-})-QDs and **2**(OH^-)-QDs) to see whether an obvious hydrogen generation could be observed. Amazingly, as shown in Fig. 2a, under the illumination of light ($\lambda > 420$ **nm**), the initial H_2 evolution rate ($r_{init.}$) of the **2**(S^{2-})-QDs **system** is increased as the increasing of the concentration of Ni^{2+} ions; while for the **2**(OH^-)-QDs system, no obvious H_2 evolution is observed with the changing of Ni^{2+} ions concentration. Besides, the employing of $NiCl_2$ could act as the similar role as that of $Ni(NO_3)_2$ (data not shown). Our results clearly demonstrate that nickel and sulfur are both essential for the catalytic reduction of proton.

We next investigated the band alignment effect of the core/shell QDs on the activity of H_2 evolution in our system. As indicated in Fig. 2a, for both **2**(S^{2-})-QDs and **1**(S^{2-})-QDs, their activity is both increased as the increasing of Ni^{2+} ions concentration. However, the activity of the system with **2**(S^{2-})-QDs ($r_{init.}$=3.39 mL h^{-1} with 400 μM Ni^{2+}) is 4.7-fold higher than that with **1**(S^{2-})-QDs ($r_{init.}$=0.72 mL h^{-1} with 400 μM Ni^{2+}). Since the overall size of **2**-QDs and **1**-QDs is nearly the same, it is rational to conclude that that the amount of S^{2-} on the surface of QDs are approximately the same. Thus, the difference lies mainly in the different band alignment of the two types of QDs, which results in the carriers accumulating dominantly in the core and shell for **1**(S^{2-})- and **2**(S^{2-})-QDs, respectively. The result therefore indicates that the tendency of the carriers migrating to the surface of QDs is vital for the high efficiency of QDs-based H_2 evolution.

We further explored the effect of the additional introduced excess S^{2-} ions (Na_2S), besides the surface-bonded S^{2-} ions, on the H_2 production activity of the system. Fig. 2b represents the activity dependence of $r_{init.}$ of the **2**(S^{2-})- and **2**(OH^-)-QDs systems under the conditions of 0.075 μM QDs, 100 μM Ni^{2+}, 0.8 M AA, pH 5.2 and $\lambda > 420$ nm on the concentration of additional introduced S^{2-} ions. As clearly shown, the activity of the systems are both increased after introducing S^{2-} ions, and the **2**(S^{2-})-QDs system exhibits the highest $r_{init.}$ of 12.1 mL h^{-1} with the ratio of Ni^{2+} to S^{2-} ($R_{Ni:S}$) at ~ 1:1; whereas the **2**(OH^-)-QDs system exhibits the highest $r_{init.}$ of 4.1 mL h^{-1} with $R_{Ni:S}$ at ~ 1:3. Assuming that the surface-bonded S^{2-} ions are densely packed on the surface of **2**(S^{2-})-QDs, the concentration of S^{2-} ions was calculated to be ~ 68 μM (see SI for details). The real $R_{Ni:S}$ of the highest $r_{init.}$ for the **2**(S^{2-})-QDs system is therefore estimated to be ~ 1:1.68. For the **2**(OH^-)-QDs system, the $r_{init.}$ is 3.3 mL h^{-1} with $R_{Ni:S}$ at 1:2, which is only slightly lower than that with $R_{Ni:S}$ at 1:3. By taking into account the experimental and calculation errors, the optimal $R_{Ni:S}$ for the highest activity of the 2-QDs systems was found to be ~ 1:2. Further increasing the concentration of S^{2-} ions has a negative effect on the H_2 production efficiency of the system. As well known, S^{2-} ions has already been demonstrated to significantly quench the photoluminescence of QDs;[26] and the reason for this is assumed to be caused by the introduction of surface traps by S^{2-} ions onto the surface of QDs. In our case, when the amount of S^{2-} ions is lower enough, it would completely complex with Ni^{2+} to form the catalyst to effectively generate H_2. However, once the amount of S^{2-} ions exceed two times of Ni^{2+} ions in the system, the excess S^{2-} ions would be left to act as trap centres which would compete with the catalyst to capture the excited electrons from QDs, and therefore results in the deficiency of the HPA system. Furthermore, our results show that the highest $r_{init.}$ of the **2**(OH^-)-QDs system is ~ 3 times lower than that of the **2**(S^{2-})-QDs system. The possible hindrance of electron transfer from QDs to the catalyst in the **2**(OH^-)-QDs system, caused by residual insulating organic ligands (Fig. S2†), is considered to response for the lower activity.

Since S^{2-} **ions** could complex with Ni^{2+} ions to form the catalyst for effective reduction **of** proton, one question is that whether other forms of sulfur precursor have the same effect as that of free S^{2-} ions. To testify this, 3-MPA, a very common thiol, was employed for comparison study. As shown in Fig. 2b, the addition of 3-MPA into the **2**(S^{2-})-QDs system exhibits the similar photocatalytic H_2 production trend as that of S^{2-} ions. Our results reveal that the H_2 production activity of the catalyst is likely irrespective of the form of sulfur precursor, but highly dependent on the $R_{Ni:S}$. The complex of nickel and sulfur with $R_{Ni:S}$=1:2, denoted as Ni-2S* (S*= S^{2-} or 3-MPA), exhibits the highest activity for our QDs-based HPA system. UV-Vis results show that no obvious change was observed before and after Ni^{2+} complexing with S^{2-} or 3-MPA (Fig. S3†), but electrochemical investigations on the solution containing Ni^{2+} (100 μM) and 3-MPA (200 μM) exhibits a cathodic feature at -0.87 V versus NHE (normal hydrogen electrode) upon the addition of acid (Fig. S4†), which is comparable with the value reported by Eisenberg and co-workers.[7] In their work, they reported that the active complex of the nickel: dihydrolipoic acid ratio is roughly 1:1, which means that the $R_{Ni:S}$ of them is also ~1:2. This result further supports our observation that the nickel and sulfur with ratio at 1:2 gives the highest activity for the reduction of proton. Despite the optimal ratio of nickel and sulfur for the highest activity of the Ni-2S* has been identified, the real structure of Ni-2S* is hard to be determined. Since the complex in solution is considered to be labile in solution,[7] and many possible nickel-containing complex structures may exist under the reaction conditions. This is evidenced by the electrospray ionization mass spectrometry (ESI-MS) analysis of the aqueous solution containing Ni^{2+} ions and 3-MPA with the molar ratio of 1:2, where complicated peaks considered corresponding to nickel-containing complex were observed (Fig. S5†).

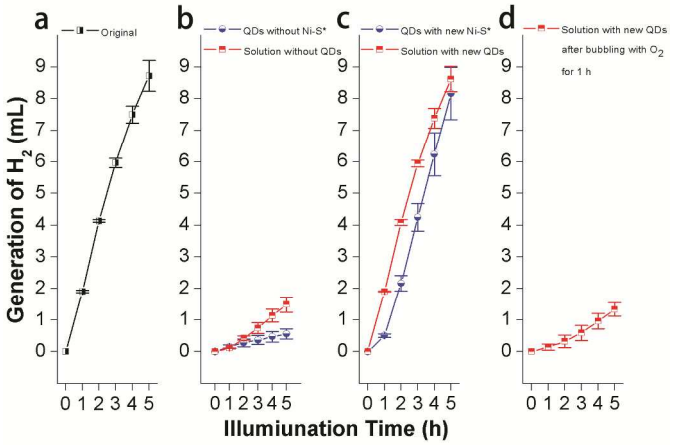

Fig. 3 H_2 generation experiments of the system with different conditions under illumination at 520 nm. **a**, the generation of H_2 of the system with **the** conditions of 0.075 μM **2**(S^{2-})-QDs, 100 μM Ni^{2+}, 100 μM 3-MPA and 0.8 M AA at pH 5.2 versus illumination time. **b**, the generation of H_2 of separated component (QDs and residual solution) with the same conditions as that of original reaction solution except without added Ni^{2+}, 3-MPA or QDs, respectively, versus illumination time. **c**, the generation of H_2 of separated component after adding new 100 μM Ni^{2+}, 100 μM 3-MPA and 0.075 μM 2(S^{2-})-QDs, respectively, versus illumination time. **d**, the generation of H_2 of the solution with new QDs after bubbling with O_2 (30 mL $min.^{-1}$) for 1h versus illumination time.

Furthermore, the H_2 evolution efficiency of the QDs system is also pH dependent with optimal pH value at 5.2 (Fig. 2c). The system with pHs lower and higher than 5.2 would exhibit **a** reduced efficiency due to the instability of QDs and the loss of donor property of AA, respectively. The stability of the QDs-based HPA system was evaluated under the conditions of 0.075 μM **2**(S^{2-})-QDs,

100 μM Ni^{2+}, 100 μM 3-MPA, and 0.8 M AA, with pH 5.2 and irradiation wavelength > 420 nm. As shown in Fig. 2d, the generation rate of H_2 is slightly reduced during the first 4 h illumination, and then kept stable at the average H_2 evolution rate ($r_{ave.}$) of ~ 5.4 mL h^{-1}. The reason for the deficiency of the activity at the initial stage is supposed as follows: for the freshly prepared QDs, it is reasonable to conclude that there should exist some active sites generated during the ligand exchange process which are considered not stable enough. Thus, as the reaction proceeds, these active sites would gradually diminish, which will result in the partial decrease of the activity of the HPA system. After 20 h successive illumination, the total generation volume of H_2 reaches 127.1 mL. Combined UV-Vis spectra, TEM and HRTEM measurements (Fig. S6 and S7,†) reveal that the structure of **2**(S^{2-})-QDs does not undergo any pronounced change after 20 h illumination. All above demonstrate the good photocatalytic stability of the QDs-based HPA system. Besides, under the same testing conditions, the H_2 evolution rate of CdS/CdSe core/shell QDs is ~ 15 times higher than that of control CdS core QDs (Fig. S8†), further demonstrating the superiority of using core/shell QDs with the proper band alignment for H_2 photogeneration than that of single component QDs.

The quantum yield (Φ) of H_2 generation was determined from the system with the conditions of 0.075 μM **2**(S^{2-})-QDs, 100 μM Ni^{2+}, 100 μM 3-MPA, 0.8 M AA, and pH 5.2 under illumination at 520 nm (Fig. 3a). It should be noted that the **2**(S^{2-})-QDs tend to aggregate in the system, though it is water-dispersible, which will apparently increase the light absorption of the system by scattering and reflection of the incident light (not contribute to the H_2 production). However, the Φ (H_2) of the system could still reach as high as 20.6 ± 1.1%. In addition, it was found that the H_2 production efficiency of the HPA system is highly wavelength dependent, which is well consistent with the absorption property of the CdS/CdSe QDs (Fig. S9†). This indicates that the H_2 evolution of the system is indeed triggered by the light absorption of the CdS/CdSe QDs.

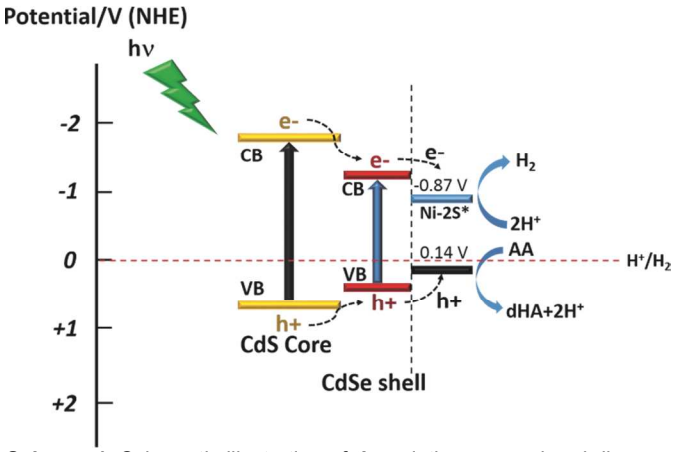

Scheme 1. Schematic illustration of **the** relative energy band diagram of **the** CdS/CdSe core/shell (**2**-QDs)-based HPA system for H_2 production in water. dHA represents dehydroascrorbic acid. Ni-2S* indicates the complex of Ni^{2+} with S^{2-} or 3-MPA. The potential value of AA changing to dHA is obtained from reference 7.

To identify whether the catalyst is on the surface of QDs or in solution, **2**(S^{2-})-QDs were separated from the reaction solution by centrifugation after 5 h illumination and reused for additional fresh H_2 generation reaction, in which each component was subjected to the same conditions (0.8 M AA, pH 5.2) except without adding new Ni^{2+}, 3-MPA or **2**(S^{2-})-QDs, respectively. As shown in Fig. 3b, significant reduction of the activity for the H_2 evolution was observed for either of the two "incomplete" reaction systems compared with that of original (complete) reaction solution. The slightly higher activity for the reaction solution without QDs originates from the residual QDs during the separation process. However, their activity could be well recovered after introducing the same concentration of new Ni^{2+}, 3-MPA or **2**(S^{2-})-QDs as that of original system, respectively (Fig. 3c). It can thus be deduced that the Ni-2S* complex that generated in the solution provides the main contribution for obtaining high photocatalytic activity of the QDs system. Further X-ray photoelectron spectroscopy and inductively coupled plasma measurement of the QDs after the photocatalytic reaction indicate that no accumulation of Ni-2S* complex on the surface of QDs after the reaction was found (**Fig. S10**†). Here it should be noted that our QDs-based HPA system shows poor resistance to O_2 passivation. As shown in Fig. 3d, after 1 h of O_2 bubbling (30 mL min^{-1}), the $r_{ave.}$ of the reaction system with new QDs is significantly reduced from 1.72 mL h^{-1} to 0.27 mL h^{-1}. Since both S^{2-} and 3-MPA could be oxidized by O_2 to form $S_2O_3^{2-}$ and disulfides,[27] respectively, we attribute this to the possible oxidation of the Ni-2S* complex by O_2, which will destroy its photocatalytic activity.

The band edge of CdS core and corresponding CdS/CdSe core/shell QDs used in our work were estimated by Tauc plots.[28] As shown in **Fig. S11**†, the band gap energy (E_g) of CdS core (3.9 nm) is 2.85 eV which is larger than its bulk material (E_g =2.4 eV[29] with the energy of CB (E_{cb}) at - 0.9 V versus NHE[30]), thus E_{cb} would shift more negative potentials due to the large quantum confinement effect.[31] After coating the 1.6 nm thick CdSe shell, the overall E_g of CdS/CdSe core/shell QDs became 2.02 eV which is still larger than that of CdSe bulk material (E_g =1.7 eV[29] with E_{cb} at - 0.6 V versus NHE[32]), therefore the negative shift of E_{cb} of CdSe would also be expected. Since the potential to reduce protons of Ni-2S* complex is 0.87 eV versus NHE, the transfer of excited electrons of QDs to the Ni-2S* complex is possible. Despite the accurate band positions of CdS/CdSe core/shell QDs cannot be determined, we could still propose the operating mechanism of our CdS/CdSe core/shell QDs-based HPA system. As indicated in Scheme 1, upon the band gap illumination, the photo-induced electron-hole pairs are generated both in the CdS core and CdSe shell. Due to the energy of CB and VB of CdSe shell lies lower and higher than that of CdS core, respectively, the excited charge carriers of CdS core will migrate to the CdSe shell, and subsequently, the electrons generated both by CdS core and CdSe shell transfer to the Ni-2S* and followed by proton reduction to H atom and finally H_2; on the other hand, the holes will oxidize AA to form dehydroascrorbic acid and protons.

Conclusions

In summary, the developing of a simple and cost-effective, but highly efficient QDs-based HPA system for the photogeneration of H_2 from water splitting is a solid step towards a green and renewable energy. Besides the band engineering of QDs to facilitate the charge carriers to migrate to the surface of QDs and improve the charge separation, the exploration of ordinary catalyst without sacrificing its activity is also crucial. We present here a significantly convenient method to obtain a cost-effective and highly efficient catalyst for solar H_2 generation from water. We have proven that not only nickel but also sulfur is indispensable for the high activity of the QDs-based catalyst and an optimal ratio of nickel and sulfur is required for the highly efficient H_2 generation. Our results and findings provide new insights into the photogeneration of H_2 of the QDs-

based artificial photosynthesis system and are expected to accelerate the process of its practical energy applications.

Acknowledgements

This work was supported by start-up funds from the Chinese Academy of Sciences (no. 110000Y163 and no. Y320711001) and the State Key Laboratory of Electroanalytical Chemistry (no. 110000R387).

Notes and references

[a] State Key Laboratory of Electroanalytical Chemistry, Changchun Institute of Applied Chemistry, Chinese Academy of Sciences, Changchun 130022, People's Republic of China. E-mail: ydjin@ciac.ac.cn

[b] Graduate University of the Chinese Academy of Sciences, Beijing 100049, People's Republic of China.

† Electronic Supplementary Information (ESI) available: Experimental details for the synthesis and ligands exchange of QDs, characterizations, calculation method of quantum yield, supplementary results and discussion. See DOI: 10.1039/c000000x/

1. J. H. Alstrum-Acevedo, M. K. Brennaman and T. J. Meyer, *Inorg. Chem.*, 2005, **44**, 6802-6827.
2. N. S. Lewis and D. G. Nocera, *Proc. Natl. Acad. Sci. U. S. A.*, 2006, **103**, 15729-15735.
3. L. Amirav and A. P. Alivisatos, *J. Phys. Chem. Lett.*, 2010, **1**, 1051-1054.
4. K. A. Brown, S. Dayal, X. Ai, G. Rumbles and P. W. King, *J. Am. Chem. Soc.*, 2010, **132**, 9672-9680.
5. K. A. Brown, M. B. Wilker, M. Boehm, G. Dukovic and P. W. King, *J. Am. Chem. Soc.*, 2012, **134**, 5627-5636.
6. A. Das, Z. Han, M. G. Haghighi and R. Eisenberg, *Proc. Natl. Acad. Sci. U. S. A.*, 2013, **110**, 16716-16723.
7. Z. Han, F. Qiu, R. Eisenberg, P. L. Holland and T. D. Krauss, *Science*, 2012, **338**, 1321-1324.
8. J. Huang, K. L. Mulfort, P. Du and L. X. Chen, *J. Am. Chem. Soc.*, 2012, **134**, 16472-16475.
9. Z. J. Li, J. J. Wang, X. B. Li, X. B. Fan, Q. Y. Meng, K. Feng, B. Chen, C. H. Tung and L. Z. Wu, *Adv. Mater.*, 2013, **25**, 6613-6618.
10. Y. Shemesh, J. E. Macdonald, G. Menagen and U. Banin, *Angew. Chem. Int. Ed.*, 2011, **50**, 1185-1189.
11. F. Wang, W. J. Liang, J. X. Jian, C. B. Li, B. Chen, C. H. Tung and L. Z. Wu, *Angew. Chem. Int. Ed.*, 2013, **52**, 8134-8138.
12. F. Wang, W. G. Wang, X. J. Wang, H. Y. Wang, C. H. Tung and L. Z. Wu, *Angew. Chem. Int. Ed.*, 2011, **50**, 3193-3197.
13. H. Zhu, N. Song, H. Lv, C. L. Hill and T. Lian, *J. Am. Chem. Soc.*, 2012, **134**, 11701-11708.
14. F. Wen, J. Yang, X. Zong, B. Ma, D. Wang and C. Li, *J. Catal.*, 2011, **281**, 318-324.
15. Z.-J. Li, X.-B. Li, J.-J. Wang, S. Yu, C.-B. Li, C.-H. Tung and L.-Z. Wu, *Energy Environ. Sci.*, 2013, **6**, 465-469.
16. A. Vaneski, J. Schneider, A. S. Susha and A. L. Rogach, *J. Photochem. Photobiol. C:Photochem. Rev.*, 2014, **19**, 52-61.
17. A. Thibert, F. A. Frame, E. Busby, M. A. Holmes, F. E. Osterloh and D. S. Larsen, *J. Phys. Chem. Lett.*, 2011, **2**, 2688-2694.
18. E. Khon, K. Lambright, R. S. Khnayzer, P. Moroz, D. Perera, E. Butaeva, S. Lambright, F. N. Castellano and M. Zamkov, *Nano Lett.*, 2013, **13**, 2016-2023.
19. M. B. Wilker, K. J. Schnitzenbaumer and G. Dukovic, *Isr. J. Chem.*, 2012, **52**, 1002-1015.
20. J. Ran, J. Zhang, J. Yu, M. Jaroniec and S. Z. Qiao, *Chem. Soc. Rev.*, 2014.
21. Z. Han and R. Eisenberg, *Acc. Chem. Res.*, 2014.
22. Z. Han, W. R. McNamara, M. S. Eum, P. L. Holland and R. Eisenberg, *Angew. Chem. Int. Ed.*, 2012, **51**, 1667-1670.
23. J. J. Li, Y. A. Wang, W. Guo, J. C. Keay, T. D. Mishima, M. B. Johnson and X. Peng, *J. Am. Chem. Soc.*, 2003, **125**, 12567-12575.
24. W. W. Yu, L. Qu, W. Guo and X. Peng, *Chem. Mater.*, 2003, **15**, 2854-2860.
25. A. Nag, D. S. Chung, D. S. Dolzhnikov, N. M. Dimitrijevic, S. Chattopadhyay, T. Shibata and D. V. Talapin, *J. Am. Chem. Soc.*, 2012, **134**, 13604-13615.
26. A. Nag, M. V. Kovalenko, J.-S. Lee, W. Liu, B. Spokoyny and D. V. Talapin, *J. Am. Chem. Soc.*, 2011, **133**, 10612-10620.
27. D. Witt, *Synthesis*, 2008, **16**, 2491-2509
28. J. Tauc, R. Grigorovici and A. Vancu, *Physica Status Solidi B*, 1966, **15**, 627-637.
29. N. Serpone and E. Pelizzetti, *Photocatalysis*, Wiley, New York, 1989.
30. A. Kudo and Y. Miseki, *Chem. Soc. Rev.*, 2009, **38**, 253-278.
31. X. Peng, M. C. Schlamp, A. V. Kadavanich and A. P. Alivisatos, *J. Am. Chem. Soc.*, 1997, **119**, 7019-7029.
32. M. Amelia, C. Lincheneau, S. Silvi and A. Credi, *Chem. Soc. Rev.*, 2012, **41**, 5728-5743.